International Journal of Fracture **98:** 1–14, 1999.

Stress intensity factor calculation based on the work of external forces

F.V. ANTUNES[1,*], J.M. FERREIRA[1] and J. BYRNE[2]
[1]*Department of Mechanical Engineering, University of Coimbra, Pólo II, 3030 Coimbra, Portugal*
[2] *Department of Mechanical and Manufacturing Engineering, University of Portsmouth, PO1 3DJ, U.K.*

Received 4 June 1998; accepted in revised form 28 January 1999

Abstract. The external forces method is a numerical method for K calculation based on the finite element method. It uses the work of the external forces W_E for the calculation of the energy release rate and is particularly advantageous when that forces are applied far from the crack front. The method was applied to a corner crack geometry with the objective of studying its accuracy. Good results were obtained for a wide range of virtual crack displacements ($0.03\% < \Delta a/a < 6\%$) considering 4 values of W_E along with a polynomial regression of order 3. For that choice of parameters the inaccuracy of K is mainly due to FEM errors. A great sensitivity of K to FEM errors was observed, however accurate values of K were obtained, with errors lower than 2 percent. So, the use of the external forces method for the calculation of K is recommended, considering its simplicity and accuracy.

Key words: Stress intensity factor, energy release rate, external forces work, finite element method.

1. Introduction

The stress intensity factor K is a parameter that characterises the magnitude of the singular stress field existing in the neighbourhood of a crack tip. It is a central concept of linear elastic fracture mechanics, being widely used in the study of brittle fracture, fatigue, stress corrosion cracking, and to some extent for creep crack growth.

Many stress intensity factor solutions are now available in the literature for cracks under quasi-static loading. However, there are many situations for which K is not available and must be calculated. Its calculation can be done using numerical methods (finite element method, boundary element method, etc.) which, due to increasing computer power, are able to solve approximately all problems.

The numerical calculation of K based on the finite element method (FEM) can be done using:

- displacement matching methods – extrapolation method (Chan et al., 1970) or singular elements based method (Ingraffea et al., 1980);
- energy based methods – total energy method (Irwin, 1958), stiffness derivative formulation (Parks, 1974; Hellen, 1975), mapping technique (DeLorenzi, 1982, 1985), J-integral method (Rice, 1968; Murakami et al., 1983), energy domain integral (Li et al., 1985; Shih et al., 1986) or crack closure integral method (Irwin, 1957; Rybicki et al., 1977; Shivakumar et al., 1988; Roeck et al., 1995).

* Corresponding author (e-mail: fernando.ventura@mail.dem.uc.pt)

In the matching methods the displacement field obtained with the FEM is compared with the analytical displacement field, which contains K in its formulation. In the energy methods, K is calculated from the energy release rate, G. In the total energy method, proposed by Irwin (1958), the total potential energy of the body is calculated for the initial and virtually extended crack using the FEM. The energy release rate is obtained directly from its definition. The stiffness derivative method also uses a virtual crack extension technique, but only the finite elements distorted by that extension are involved in the analysis. It is now outdated, but it was the precursor to the modern approaches. DeLorenzi (1982, 1985) improved this method by calculating G from a continuum mechanics viewpoint. This methodology for G calculation is not restricted to the FEM, in opposition to the stiffness derivative approach which was developed solely through a finite element approach. The J-integral method is an alternative technique, however the evaluation of pointwise values is difficult in three-dimensional cracked bodies. More recent formulations of J (Li et al., 1985; Shih et al., 1986) apply a volume integration, that provides much better accuracy and are much easier to implement numerically. Finally, in the crack closure integral method, first proposed by Irwin (1957), G is estimated considering a crack extension and evaluating the work done to close the crack to the original configuration. In order to avoid the need of two FEM analysis, Rybicki et al. (1977) used the nodal forces ahead of the crack tip and the displacements behind it. Shivakumar et al. (1988) and Roeck et al. (1995) extended the formulation for three-dimensional problems.

The objective of the present work is to study the calculation of K based on the total energy method. Since the work of external forces is used to calculate the energy release rate of the cracked body, the method can be called the external forces method (EFM). This method is very simple and is particularly advantageous when the external forces act far from the crack front. In that case, the quantities involved in the analysis are not much affected by the difficulties of the FEM simulating the $1/\sqrt{r}$ stress singularity existing near the crack front. The method was applied to a corner crack geometry and the accuracy of K-values was studied. A comparison was made with the extrapolation method and with the crack closure integral method.

2. *K* calculation using the external forces method

In this method the calculation of K is done in an indirect way from the energy release rate G according to the relationship

$$K = \sqrt{\frac{EG}{1-\nu^2}}, \tag{1}$$

where E is the Young's modulus and ν is Poisson's ratio. This relationship is valid for plane strain conditions (for plane stress condition $K = \sqrt{EG}$). Usually a plane strain condition is assumed along the whole crack front, except at the free surfaces where a plane stress situation is assumed. However, Bakker (1992) stated that a plane strain state exists in the limit $r \to 0$ along all the crack front, so K should be always calculated using (1).

G is the derivative of the potential energy of the body with respect to crack area, for fixed load or fixed displacements

$$G = -\frac{\mathrm{d}\pi}{\mathrm{d}A}, \tag{2}$$

where π is the potential energy of the loaded body and $\mathrm{d}A$ is a virtual crack increment. This quantity is physically meaningful as it can be considered the crack driving force. If the

infinitesimal crack increment $\mathrm{d}A$ is confined to a zone of the crack front G is a local value and a distribution of G can be obtained along the crack front. The crack increment must be in the plane of the crack and normal to the crack front, because this is expected to be the easiest path for the crack in a homogeneous and isotropic material. When the virtual crack increment occurs uniformly along all the crack front and in the plane of the crack, G is a mean value.

The potential energy for a cracked body, statically loaded with point, surface and body forces, $\{F\}_p$, $\{F\}_S$, $\{F\}_b$, respectively, is given by

$$\pi = \int_V \tfrac{1}{2}\{\boldsymbol{\sigma}\}^T\{\boldsymbol{\varepsilon}\}\,\mathrm{d}V - \{\mathbf{u}\}^T \cdot \{F\}_p - \int_S \{\mathbf{u}\}^T \cdot \{F\}_S\,\mathrm{d}S - \int_V \{\mathbf{u}\}^T \cdot \{F\}_b\,\mathrm{d}V, \tag{3}$$

where $\{\boldsymbol{\sigma}\}$, $\{\boldsymbol{\varepsilon}\}$ and $\{\mathbf{u}\}$ are the stress, strain and displacement vectors, respectively, V is the volume of the body and S its surface. The first term is the elastic deformation energy of the body U and the last three terms are the potential of the external forces. According to this expression, the energy available for crack extension (energy release rate) has two sources: the work of applied external forces and the energy stored in the body. According to the principle of energy conservation (1st law of thermodynamics), the work performed by the external forces in an adiabatic and reversible way, is stored as deformation energy in the body (U). Since the work done by the external forces acting on a body is given by

$$W_E = \tfrac{1}{2}\{\mathbf{u}\}^T \cdot \{F\}_p + \int_S \tfrac{1}{2}\{\mathbf{u}\}^T \cdot \{F\}_S\,\mathrm{d}S + \int_V \tfrac{1}{2}\{\mathbf{u}\}^T \cdot \{F\}_b\,\mathrm{d}V, \tag{4}$$

the potential energy is

$$\pi = -W_E. \tag{5}$$

So, G is also given by

$$G = \frac{\mathrm{d}W_E}{\mathrm{d}A}. \tag{6}$$

This derivative can be approximately calculated considering two values of W_E for the initial and extended virtual crack areas A and $A + \Delta A$

$$G \approx \frac{\Delta W_E}{\Delta A}. \tag{7}$$

The error of this approximation increases with the virtual crack increment ΔA. Antunes (1993) in a two-dimensional analysis obtained good results with crack increments less than 15 percent of the crack length. An alternative solution proposed was to consider the virtual crack extensions $-\Delta A$ and $+\Delta A$, and calculate G doing

$$G \approx \frac{(W_E)_{A+\Delta A} - (W_E)_{A-\Delta A}}{2\Delta A} \tag{8}$$

The results obtained were clearly better than the ones given by (7). However, the best solution is to consider several values of W_E for different virtual crack increments, as Figure 1 shows, fit a polynomial curve to the results by regression and obtain the derivative of that polynomial for

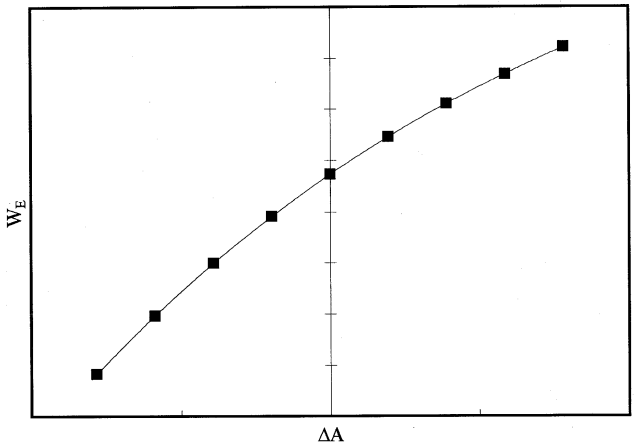

Figure 1. Plot of W_E versus ΔA for G calculation.

$\Delta A = 0$. The accuracy of K increases in general with the number of virtual crack increments considered, but this means an increase in the computational effort.

The values of W_E can be obtained numerically using the finite element method (FEM). Since in the FEM the external forces are replaced by equivalent nodal forces, the work of external forces is given by

$$W_E = \sum_{i=1}^{NN} \tfrac{1}{2}(F_x u + F_y v + F_z w)_i, \tag{9}$$

where NN is the number of nodes, $(F_x, F_y, F_z)_i$ are the Cartesian components of the nodal force on node i (directly applied or reaction) and $(u, v, w)_i$ are the displacements of the same node.

2.1. Advantages and disadvantages of the method

The methodology presented for K calculation is very simple, so can be easily implemented. The only results of the FEM needed are the nodal displacements and the nodal forces. Since the nodal displacements are the primary variables of the FEM analysis, they are the most accurate results of this method. A great advantage is obtained when the external loads act far from the crack front, or acting close to it do not produce work. In this case, the nodal displacements close to the crack front, which are the most affected by simulation difficulties of the crack singularity, are not necessary.

An important disadvantage of the EFM is that it needs more than one FEM analysis to calculate K, while with other methods only one analysis is necessary. This is particularly important when K is to be obtained at several positions along a crack front. When local K-values are sought, these are affected by the extension of crack front involved in the virtual crack propagation. To obtain a pointwise G an infinitesimal crack extension, extending over an infinitesimal crack front segment, in the plane of the crack and in the direction normal to the crack front should be considered. However, since ΔA extends over a finite extension of the crack front in the vicinity of the point under study, a local weighted average value of G is obtained. The approach used also does not account for the fact that, in general, the direction

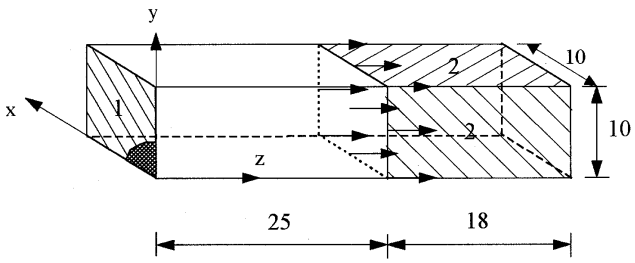

Figure 2. Corner crack geometry (surface 1: restriction to movement along z; surfaces 2: restrictions to movement along x and y).

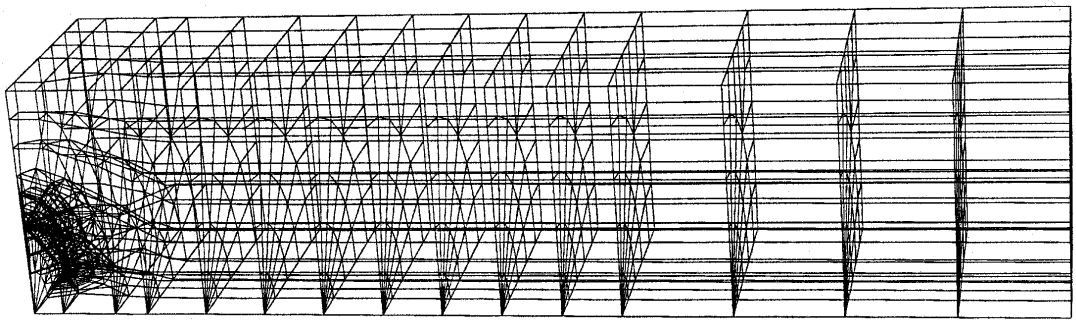

Figure 3. Finite element mesh.

of the local virtual crack extension does not coincide with that of the local energy release rate. Finally, the method is not adequate to study mixed mode problems, because separate K-values cannot be obtained.

3. Application of the method to a corner crack geometry

3.1. THE CORNER CRACK GEOMETRY

For the study of K calculation based on the EFM, the corner crack (CC) geometry presented in Figure 2 was considered. The body is tension loaded, so mode I loading exists along the whole crack front. The load is static and a magnitude of 60 kN was considered, that corresponds to a remote stress of 600 MPa. The boundary conditions are also indicated in Figure 2. There are restrictions to z movement at the cracked section and to x, y movement at the head of the body, so the problem of rigid body movement does not exist in the FEM analysis. The restrictions at the head restrain its rotation and bending. The material was considered continuous, homogeneous, isotropic and with linear elastic behaviour. The elastic properties considered were $E = 1.7 \times 10^{11}$ Pa (Young's Modulus) and $\nu = 0.3$ (Poisson's ratio).

The FEM code used was MODULEF (INRIA, 1987). The division of the cracked body of Figure 2 into a mesh of finite elements was done considering quadratic isoparametric elements: 20-node hexaedric elements and 15-node pentaedric elements (Onãte, 1992). At the crack front, singular pentaedric elements with 15 nodes were used, in which the desired singularity $(1/\sqrt{r})$ is achieved moving the mid-side nodes to quarter-point positions (Freese et al., 1976; Banks-Sills et al., 1989). A full Gaussian numerical scheme was used for these elements ($3 \times 3 \times 3$ integration points for the 20-node element, and 21 points for the 15-node

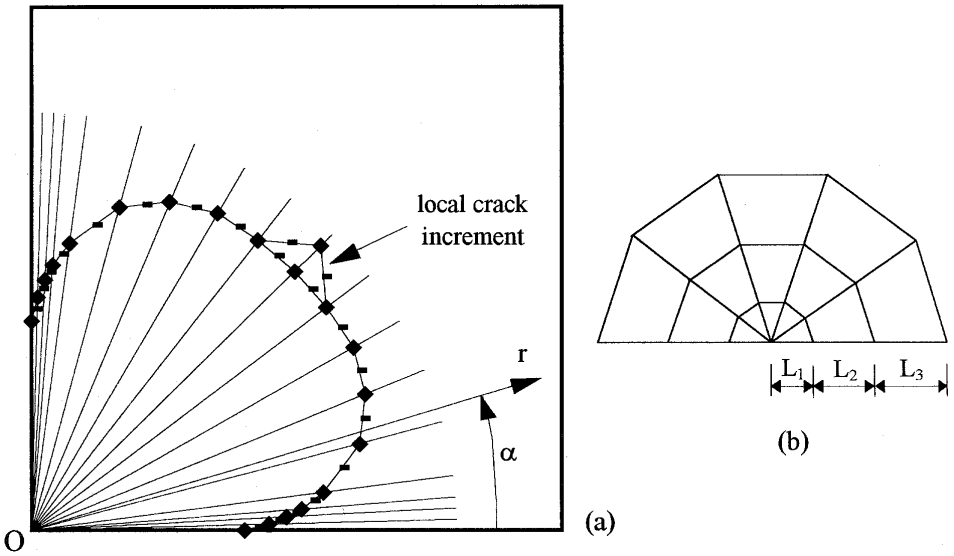

Figure 4. (a) Distribution of nodes along the crack front; (b) spider web mesh around each crack front point.

element). Figure 3 shows the finite element mesh considered for a quarter-circular crack with 5 mm, which has 3930 nodes and 861 elements. This mesh was changed for different dimensions and shapes of the crack, however the number of elements and nodes was maintained constant. It has three main parts; a spider web mesh around the crack front, a transition mesh and a regular mesh far from the crack front, with 270, 195 and 396 elements, respectively. Special care was taken in the definition of the spider web mesh, because the errors of the FEM arise mainly due to the difficulty of simulation of the singularity existing around the crack front. In the direction longitudinal to the crack front 18 elements were considered, with a total number of 37 nodes, as shown in Figure 4(a). The angular distribution of elements is more refined near the surface, to account for boundary layer effects. The geometry of the spider web around each crack front point can be seen in Figure 4(b).

The virtual crack displacement of the corner nodes was made always along a direction α, as indicated in Figure 4(a). The movement of the two mid-side node neighbours of the corner node displaced was half of the displacement of the corner node, as represented in the same figure. The crack increment was accomplished by a repositioning of the quarter-point nodes, in order to maintain the simulation of the singularity $r^{-1/2}$.

3.2. ACCURACY OF K-VALUES

During K calculation there are several approximations that affect its accuracy. Naturally it is important to have correct values. K results can be considered satisfactory when the error is within the range 5–10 percent, since material toughness has normally a great spread. When K-values are used in fatigue, a better accuracy is required, due to fatigue crack propagation laws. In these, ΔK appears to power 2 or greater, so an accuracy of 1–2 percent is necessary, if possible. The accuracy of the results obtained with the EFM was studied and the results are presented next.

In the EFM the effective relation existing between W_E and A (crack area) is approximately defined considering several virtual crack increments and fitting a regression curve to the nu-

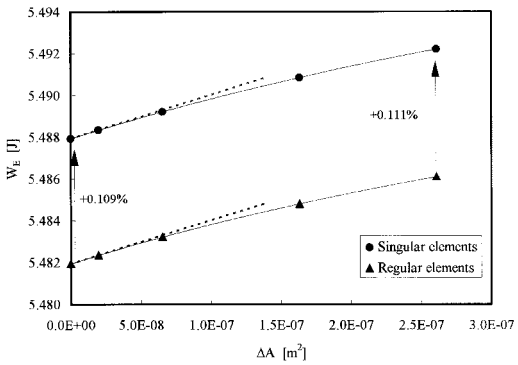

Figure 5. Influence of FEM errors on the accuracy of K.

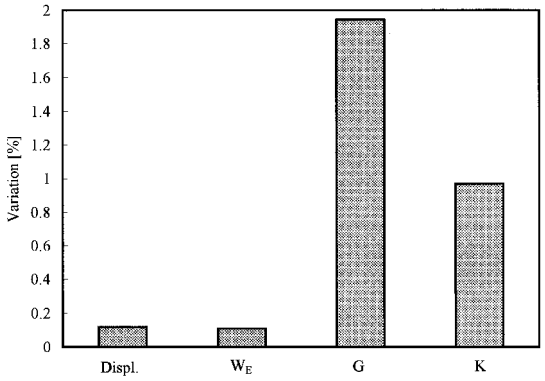

Figure 6. Percentage variation of displacements, W_E, G and K, produced by the replacement of regular elements by natural singular elements at the crack front.

merical values of W_E, as indicated in Figure 1. The error associated with this approximation depends on: accuracy of nodal displacements (i.e., accuracy of data), number of virtual crack increments, values of ΔA and regression curve used for fitting the values of W_E.

3.2.1. *Influence of FEM errors on the accuracy of K*

In the FEM the accuracy depends on the capacity of the finite elements to simulate the real displacement field, so the parameters are: the finite element mesh (the distribution of elements along and around the crack front being particularly important); the type of elements and the order of integration of element matrices. In the present mesh only the mesh can be varied, because the other parameters have already been defined. Small variations of the external forces work (W_E) were obtained, less than 0.1 percent, for a wide range of finite element dimensions, which indicates a good accuracy. This good accuracy is explained by the remote location of the nodes involved in the calculation of W_E relative to the crack front, where the FEM performs worst.

Although the estimation of W_E is very accurate, the small errors that inevitably exist influence the accuracy of K-values. If the FEM errors were zero, the values of W_E would be correct and G would not be affected. This would also happen if the several values of W_E had identical errors, because the curve W_E/A (see Figure 1), would only be translated without rotation. In fact, the slope of tangent at $\Delta A = 0$, i.e. G would not be affected because the FEM errors would cancel. However, the virtual crack increments produce always a change in the accuracy of the FEM, so the curve W_E/A has always a small rotation in relation to its correct angular position. If the virtual crack increments produce an improvement of FEM accuracy, the curve W_E/A is rotated anti-clockwise and K is higher than its correct value. On the other hand, a decrease of accuracy with the virtual crack increments produces lower K-values. So, the influence of FEM errors on the accuracy of G is due to different errors existing before and after virtual crack increment, and not due to the errors themselves.

Figure 5 shows the variation of the curve $W_E/\Delta A$ when regular elements are replaced by singular elements at the crack front of a quarter-circular crack with 5 mm radius. For $\Delta A = 0$, the variation of W_E is 0.109 percent, while for $\Delta A = 2.6 \times 10^{-7}\,\mathrm{m}^2$ this variation is slightly

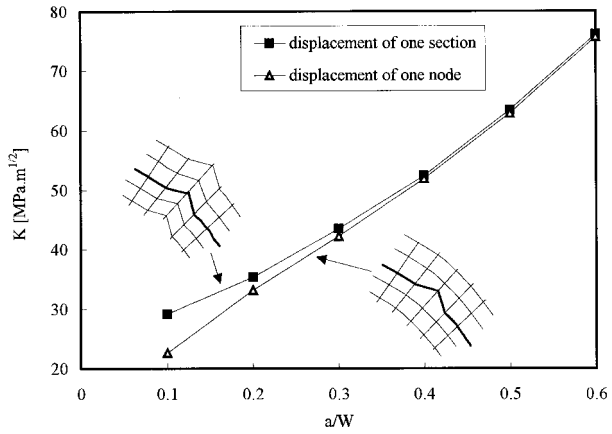

Figure 7. Influence of the way the virtual crack increment is produced.

higher (0.111 percent). This higher variation of W_E indicates that the FEM errors are higher for the crack virtually extended, which means that the virtual increment produces a finite element mesh that gives worse results than the initial mesh. The FEM errors rotate the curve $W_E/\Delta A$ clockwise, giving a G-value lower than its correct value. The improvement of FEM analysis with the use of singular elements at the crack front produces a rotation of $W_E/\Delta A$ anti-clockwise, approaching G to its correct value. The improvement of FEM results reduces the error in G because the variation of accuracy with virtual crack increment is attenuated. The variation of G in Figure 5 is 1.94 percent, so one order of magnitude higher than the variation of W_E. This means that the derivative of W_E amplifies its error. The influence of FEM errors during K calculation procedure can be visualised in Figure 6. This figure shows the variations of displacements, W_E, G and K produced by the replacement of regular elements by singular elements at the crack front, for a quarter-circular crack with 5 mm radius. It can be seen that the variations in displacements and W_E are very small, which indicates that they are very accurate. However, the variation in G is significantly higher, which indicates the important influence that small errors of W_E can have on G. Finally, the variation of K is slightly smaller than the variation of G. It is evident that the accuracy of K is very sensitive to FEM errors.

An interesting result was obtained for quarter-circular cracks. It was observed that when the virtual crack increment is produced by displacing only the crack front node the results are lower than when the increment is produced by displacing one section of the spider web. The results presented in Figure 7 show that the difference reduces with crack length, being 29 percent for $a = 1$ mm and 0.6 percent for $a = 6$ mm. This is explained by the different changes in the accuracy of the FEM produced by the two virtual crack increments. In fact, when all the spider web section is displaced, this affects the size of elements in the transition mesh, which is the main source of FEM errors for cracks with small length. In this case, associated with the virtual crack increment there is an important change of the accuracy. Since the virtual crack increment produces an improvement of FEM results, K-values are higher than the correct values. The displacement of the crack front node produces a distortion only of the crack front elements, which has a lower effect on the accuracy of the FEM. For higher crack lengths, the influence of the size of elements in the transition mesh reduces, so the differences between the two virtual propagation modes are lower. This reinforces the idea that the changes produced by the virtual crack increments in the accuracy of FEM must be as small as possible.

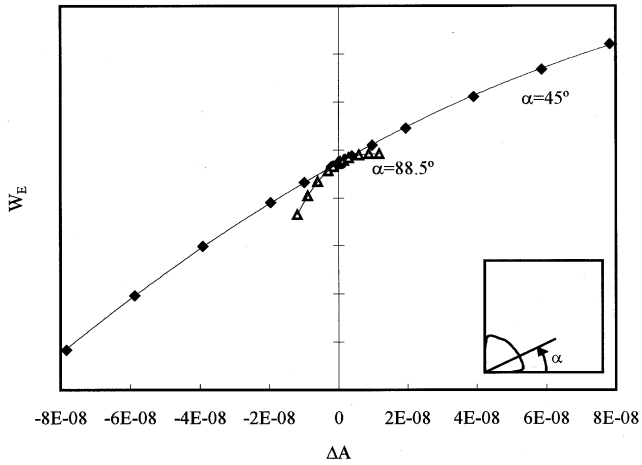

Figure 8. W_E values for different virtual crack increments at points $\alpha = 45°$ and $\alpha = 88.5°$.

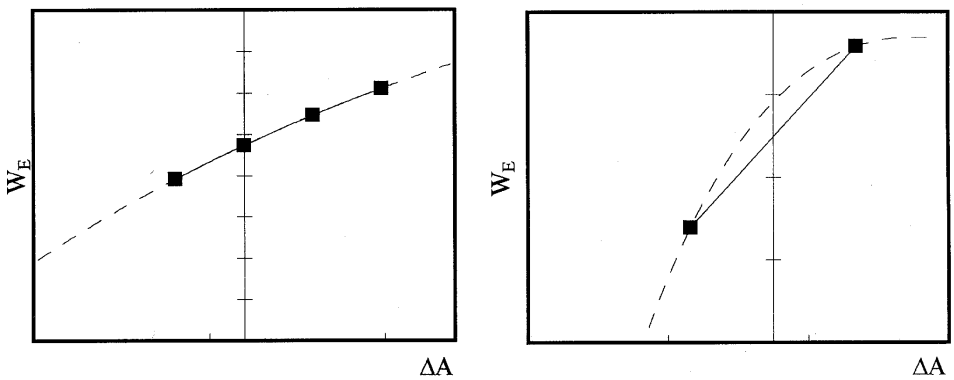

Figure 9. Calculation of G using (a) 4 values of W_E; (b) 2 values of W_E.

3.2.2. *Influence of virtual crack increments and regression curve*

The accuracy of K is also influenced by the number of virtual increments, by the magnitude of that increments (ΔA) and by the regression curve used to fit the results. Figure 8 presents the results obtained for the crack front points $\alpha = 45°$ and $\alpha = 88.5°$ of the crack represented, considering local virtual crack increments. The spider web mesh used had dimensions $L_1/a =$ 20 percent, $L_2/a = 5$ percent, $L_3/a = 6.6$ percent (see Figure 4(b)), where $\underline{a}$ is the crack length for $\alpha = 45°$. For $\alpha = 88.5°$, the range of ΔA is lower than for $\alpha = 45°$, although the virtual displacements (Δa) of the crack front nodes are the same. In general, two aspects influence the relation existing between Δa and ΔA: the extent of crack front involved in virtual crack increment and the direction of virtual displacement relatively to the crack front. In the case presented in Figure 8, for $\alpha = 45°$ the crack increment is normal to the crack front, while for $\alpha = 88.5°$ this does not happen due to the tunnelling effect, which reduces ΔA for the same Δa. It can also be seen in Figure 8 that the concavity of the plots W_E versus ΔA is negative and is more important for $\alpha = 88.5°$. The concavity can affect the accuracy of K because with the increase of concavity, the correct definition of the curve $W_E/\Delta A$ is difficulted. This concavity depends on Δa, increasing with it.

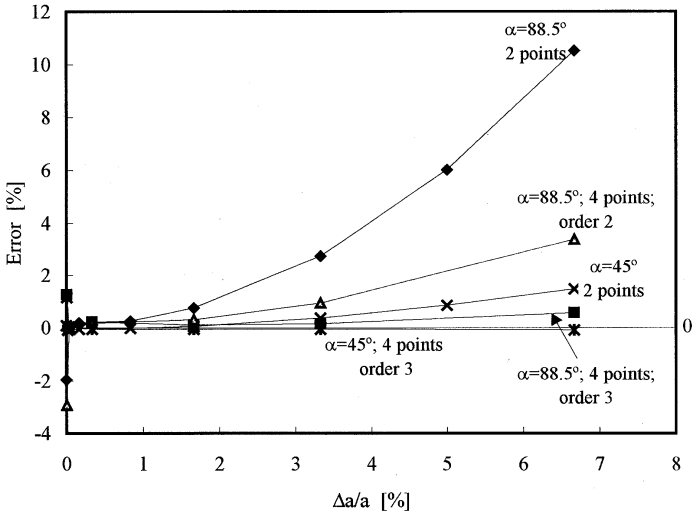

Figure 10. Errors of K for different Δa and number of points (2 or 4).

The accuracy of the relation W_E versus A is expected to increase with the number of virtual crack increments considered, however this means an increase in the computational effort involved. In the two cases presented in Figure 8, 17 values of W_E were considered, which enable a good approximation to the real relation existing between W_E and ΔA. However, it is not possible always to consider so many points, so the two options presented in Figures 9(a) and 9(b) were assumed. In the first case, 4 values of W_E are considered, one corresponding to the initial crack ($\Delta A = 0$) and the others corresponding to virtual crack increments $-\Delta A$, ΔA and $2\Delta A$. The relation W_E versus ΔA can be approximately defined from the 4 points using a polynomial regression of order 2 or 3. In the alternative solution presented in Figure 9(b), only two symmetrical virtual increments, ΔA and $-\Delta A$ are considered. In this case, G is approximately given by the slope of the straight line defined by these two values, according to (8). This option has the advantage of requiring only two FEM analysis, instead of the four necessary in the other option. The dashed curves presented in Figures 9(a) and 9(b) are the 'correct' curves obtained with 17 points, as Figure 8 shows.

In Figure 10, the accuracy obtained with these solutions can be compared. The values considered as correct were obtained with 17 points and a polynomial regression of order 3, as indicated in Figure 8. It can be seen that the consideration of 4 points gives better results than the consideration of 2 points. With 4 points, better results are obtained considering a polynomial of order 3. The use of 2 points gives good results if relatively small virtual increments are considered. Near the surface ($\alpha = 88.5°$) the results are worse than for $\alpha = 45°$, whether 4 or 2 points are used. This can be attributed to the higher concavity of the relation W_E versus ΔA.

Higher virtual crack displacements (Δa) produce worse results, so small virtual crack increments must be used. This can be explained by an increasing effect of the distortion produced in the finite element mesh by the virtual crack increment. It can also be related to the concavity of the W_E versus ΔA relation, because higher concavities are expected to give worse results. On the other hand, Δa cannot be so small that the change of W_E is not adequately measured, due to the limitations existing in the representation of numbers by the computer. This effect was observed for $\Delta a/a < 0.002$ percent. In the selection of Δa, the

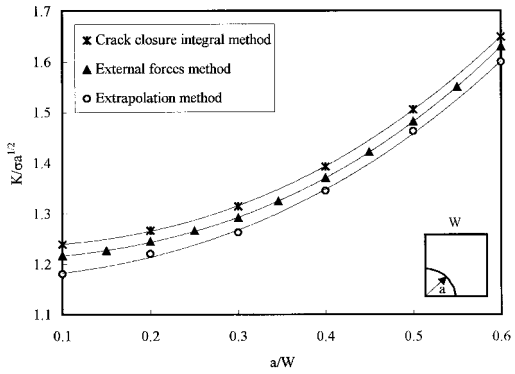

Figure 11. Comparison between results obtained for quarter-circular cracks using the EFM and other methods of K calculation.

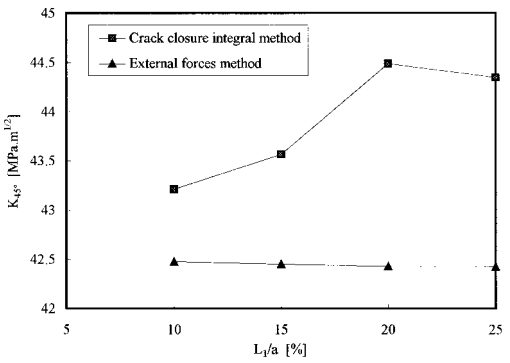

Figure 12. Variation of K_{45° with the size of crack front elements (L_1) for a quarter-circular crack with 3 mm.

dimension of crack front elements must also be considered, so that the distortion due to that increment is not exaggerated.

According to the results presented in Figure 10, very accurate results are obtained with 4 points and an order of regression 3 for a wide range of virtual crack increments. For $0.03\% < \Delta a/a < 6\%$, the maximum errors obtained were 0.08 percent for $\alpha = 45^\circ$ and 0.5 percent for $\alpha = 88.5^\circ$. In that case, the errors of K are mainly due to FEM errors. An accuracy of approximately 2 percent is expected to be obtained with the EFM if the parameters that influence it are correctly chosen.

3.3. Comparison with other methods

The extrapolation method (Chan et al., 1970) and the crack closure integral method (Rybicki et al., 1977; Shivakumar et al., 1988) were used to validate the results obtained with the EFM. That methods have the advantage of needing only one FEM analysis, in opposition to the EFM which needs more than one analysis to obtain a K-value. Figure 11 presents the results obtained for the crack front point $\alpha = 45^\circ$ of quarter-circular cracks with different lengths. The K-values obtained with the EFM are between the results obtained with the other two methods. The differences between the EFM and each of the other methods are lower than 2 percent, which is a good indication for its accuracy.

The results presented in Figure 11 were obtained for $L_1/a = 10$ percent, where L_1 is the radial size of the crack front elements and $\underline{a}$ is the crack length. Figure 12 shows the values of K obtained with crack front elements of different sizes (L_1) for a quarter-circular crack with $a = 3$ mm. It can be seen that the crack closure integral method is much more sensitive to L_1 than the EFM, which indicates that it is more affected by errors. In fact, the crack closure integral method uses results of the FEM (nodal displacements and nodal reactions) close to the crack front, which are the most affected by errors. Rybicki and Kanninen (1977) did a two-dimensional analysis of a finite plate with a central crack and obtained accuracies within 6 percent of the reference solution for values of L_1 up to 20 percent of the crack length. The extrapolation method is also expected to be less accurate than the EFM because it uses FEM results relatively close to the crack front.

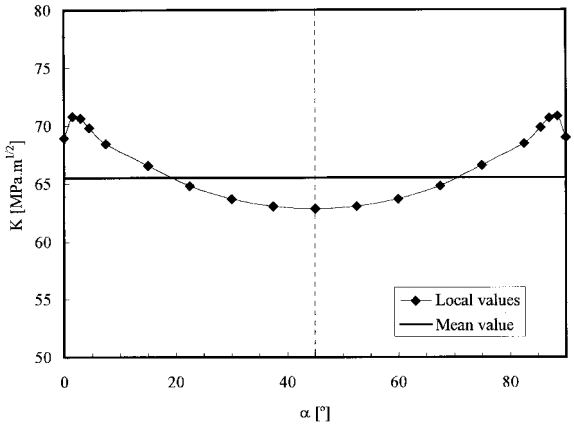

Figure 13. K distribution along the crack front of a quarter-circular crack with a length of 5 mm.

In conclusion, the EFM can be recommended for the calculation of K instead of the other two methods analysed here. The crack closure integral method is adequate for the study of mixed mode problems.

3.4. K-VALUES ALONG A QUARTER-CIRCULAR CRACK FRONT

The K distribution along the crack front of a quarter-circular crack with 5 mm length is presented in Figure 13. This distribution is symmetric in relation to $\alpha = 45°$, which was expected since the physical problem is symmetric in relation to that plane. The mean K-value is represented and is also qualitatively correct.

It can be seen that K is not constant along the crack front, having a variation of 10 percent for the crack studied. The lowest value is obtained for $\alpha = 45°$ and an increase is observed from there to the free surfaces. However, a decrease is observed near the surface, which is explained by the weaker singularity of the stress field existing at the corner points. In fact, since the crack/surface angle is $\beta = 90°$ and $\nu = 0.3$, the singularity is $r^{-\lambda}$ with $\lambda < 0.5$ and K should be zero (Benthem, 1977; Bazant et al., 1979; Leung et al., 1996), because this is defined as the magnitude of the singularity $r^{-0.5}$. However, values obtained are finite and of the same order as elsewhere along the crack front. This indicates that the surface values have not converged to their correct values because the finite elements used near the corner points cannot model the discontinuity of K along the crack front. In fact, the elements used can only accommodate a quadratic variation of displacements and the region in which K reduces to zero from its near surface value has a small extent. The method used for K calculation also explains the finite value at the surface. In fact, a virtual crack increment extending over the crack front is considered, so K is not a pointwise value but a weighted average that includes all the crack front points involved. This way, the K-value obtained at the surface is increased by the near surface nonzero values. The mesh refinement near the surface along the thickness direction, would reduce the surface value of K. So, K surface values, although finite and of the same order as elsewhere, cannot be considered valid. The difficulties of the FEM near the surface are not expected to affect the results for the interior crack front. In fact, Bakker (1992) observed that only the calculated free surface value of K was affected by the mesh refinement in the thickness direction, while the effect at interior crack front points was negligibly small.

4. Conclusions

The main conclusions are:

- the external forces method (EFM) can be easily implemented as it only needs the nodal displacements and nodal forces resulting from the finite element method (FEM). It is particularly advantageous when the external forces are applied far from the crack front, or acting there do not produce work;
- the accuracy of K-values is very sensitive to the accuracy of the FEM results. The influence of FEM errors on K is due to the variation of the accuracy of the FEM produced by the virtual crack increments. This way, the distortion produced by the virtual crack increment on the finite element mesh must be as small as possible;
- for K calculation, the consideration of 4 values of W_E along with a polynomial regression of order 3 gives good results for a wide range of virtual crack displacements ($0.03\% < \Delta a/a < 6\%$). For this choice of parameters, the inaccuracy of K is mainly due to FEM errors;
- accurate results, with an error lower than 2 percent, can be obtained for K if the different parameters are adequately defined. However, higher errors are obtained for corner points;
- due to its simplicity and accuracy, the EFM can be recommended for the calculation of stress intensity factors in two- and three-dimensional situations.

References

Antunes, F.J.V. (1993). *Use of Finite Element Method in The Calculation of Stress Intensity Factors*, Master Thesis, Department of Mechanical Engineering, University of Coimbra. (In Portuguese)

Bakker, A. (1992). Three-dimensional constraint effects on stress intensity distributions in plate geometries with through-thickness cracks. *Fatigue and Fracture of Engineering Materials and Structures* **15**(11), 1051–1069.

Banks-Sills, L. and Sherman, D. (1989). On quarter-point three-dimensional finite elements in linear elastic fracture mechanics. *International Journal of Fracture* **41**, 177–196.

Bazant, Z.P. and Estenssoro, L.F. (1979). Surface singularity and crack propagation. *International Journal of Solids and Structures* **15**, 405–426.

Benthem, J.B. (1977). State of stress at the vertex of a quarter-infinite crack in a half-space. *International Journal of Solids and Structures* **13**, 479–492.

Chan, S.K., Tuba, I.S. and Wilson, W.K. (1970). On the finite element method in linear fracture mechanics. *Engineering Fracture Mechanics* **2**, 1–17.

DeLorenzi, H.G. (1982). On the energy release rate and the J-Integral for 3-D Crack Configurations. *International Journal of Fracture* **19**, 183–193.

DeLorenzi, H.G. (1985). Energy release rate calculations by the finite element method. *Engineering Fracture Mechanics* **21**(1), 129–143.

Freese, C.E. and Tracey, D.M. (1976). The natural isoparametric triangle versus collapsed quadrilateral for elastic crack analysis. *International Journal of Fracture* **12**, 767–770.

Hellen, T.K. (1975). On the method of virtual crack extension. *International Journal for Numerical Methods in Engineering* **9**, 187–207.

Ingraffea, A.R. and Manu, C. (1980). Stress-intensity factor computation in three dimensions with quarter-point elements. *International Journal for Numerical Methods in Engineering* **15**, 1427–1445.

INRIA (Institut National de Recherche en Informatique et en Automatique) (1987). *Presentation of Club Module F*, Le Chesnay, France. (In French)

Irwin, G.R. (1957). Analysis of stresses and strains near the end of a crack transversing a plate. *Journal of Applied Mechanics* **24**, 361–364.

Irwin, G.R. (1958). Fracture. *Encyclopedia of Physics* **4**, Springer, Berlin.

Leung, A.Y.T. and Su, R.K.L. (1996). Analytical solution for mode I crack orthogonal to free surface. *International Journal of Fracture* **76**, 79–95.

Li, F.Z., Shih, C.F. and Needleman, A. (1985). A comparison of methods for calculating energy release rates. *Engineering Fracture Mechanics* **21**(2), 405–421.

Murakami, T.K. and Sato, T. (1983). Three-dimensional J-integral calculations of part-through surface crack problems. *Computers and Structures* **17**, 731–736.

Oñate, E. (1992). *Finite Element Method Calculation of Structures – Static Linear Analysis*, Centro Internacional de Métodos Numéricos en Ingeniería, Barcelona. (In Spanish)

Parks, D.M. (1974). A stiffness derivative finite element technique for determination of crack tip stress intensity factors. *International Journal of Fracture* **10**, 487–502.

Rice, J.R. (1968). A path independent integral and approximate analysis of strain concentration by notches and cracks. *Journal of Applied Mechanics* **35**, 379–386.

Roeck, G. and Wahab, M.M.A. (1995). Strain energy release rate formulae for 3D finite element. *Engineering Fracture Mechanics* **50**(4), 569–580.

Rybicki, E.F. and Kanninen, M.F. (1977). A finite element calculation of stress intensity factors by a modified crack closure integral. *Engineering Fracture Mechanics* **9**, 931–938.

Shih, C.F., Moran, B. and Nakamura, T. (1986). Energy release rate along a three-dimensional crack front in a thermally stressed body. *International Journal of Fracture* **30**, 79–102.

Shivakumar, K.N., Tan, P.W. and Newman Jr., J.C. (1988). A virtual crack-closure technique for calculating stress intensity factors for cracked three dimensional bodies. *International Journal of Fracture* **36**, R43–R50.